EUSIPCO-94
VII European Signal Processing Conference
September 13-16, 1994 Edinburgh, Scotland

A TIME AND SLOPE DOMAIN THEORY OF MORPHOLOGICAL SYSTEMS: SLOPE TRANSFORMS AND MAX–MIN DYNAMICS

Petros Maragos

School of Electrical & Computer Engineering
Georgia Institute of Technology, Atlanta, GA 30332–0250, USA

ABSTRACT

In this paper we present a theory for a broad class of nonlinear systems obeying a supremum/infimum-of-sums superposition and a collection of related analytic tools, which parallel the functionality of and have many conceptual similarities with ideas and tools used in linear systems. In the time domain, the equivalence of these systems with morphological dilation or erosion by their impulse response is established, and a class of nonlinear (max–min) difference equations is introduced to describe their dynamics. Finding that the affine signals $\alpha t + b$ are eigenfunctions of such morphological systems leads to developing a slope response for them, as a function of the slope α, and related slope transforms for arbitrary signals. These ideas provide a transform (slope) domain for morphological systems, where dilation and erosion in time corresponds to addition of slope transforms, time lines transform into slope impulses, and time cones transform into bandpass slope-selective filters.

1. MORPHOLOGICAL SYSTEMS

Morphological systems have found many applications in image analysis and nonlinear filtering. All are based on (simple or complex) parallel or serial interconnections of morphological dilations $\oplus$ or morphological erosions $\ominus$ [7, 6]

$$(x\oplus g)(t) = \bigvee_{\tau} x(\tau)+g(t-\tau) \quad , \quad (x\ominus g)(t) = \bigwedge_{\tau} x(\tau)-g(\tau-t)$$

where $\bigvee$ denotes supremum and $\bigwedge$ denotes infimum. So far their analysis has been done only in the time domain by using their algebraic properties and lacked a transform domain.

In this paper we first endow morphological systems with various concepts and analytic methods that enable us to determine their output and several properties of these nonlinear systems in the time domain based on their *impulse response*. Specifically, we call a signal operator $\mathcal{D} : x \mapsto y = \mathcal{D}(x)$ a *dilation translation-invariant (DTI)* system if it is time-invariant and obeys the morphological *supremum superposition* principle ($c_i \in \mathbf{R}$)

$$\mathcal{D}\left[\bigvee_i c_i + x_i(t)\right] = \bigvee_i c_i + \mathcal{D}[x_i(t)] \qquad (1)$$

For DTI systems we assume input and output signals $x : \mathrm{E} \to \overline{\mathbf{R}}$ with a continuous (E=R) or discrete domain (E= Z) and whose range is any subset of $\overline{\mathbf{R}} = \mathbf{R} \cup \{-\infty, \infty\}$. The useful information in a signal x analyzed by a DTI system exists only at times t in its *support* $\mathrm{Spt}(x) = \{t : x(t) > -\infty\}$. The morphological *zero impulse* μ and *zero step* λ

$$\mu(t) \triangleq \begin{cases} 0, & t=0 \\ -\infty, & t \neq 0 \end{cases} \quad , \quad \lambda(t) \triangleq \begin{cases} 0, & t \geq 0 \\ -\infty, & t < 0 \end{cases}$$

are two elementary signals useful for analyzing morphological systems. For example, the *impulse response* $g(t) = \mathcal{D}[\mu(t)]$ uniquely characterizes a DTI system in the time domain and determines its causality and stability. Specifically [4]

$$\mathcal{D} \text{ is DTI} \iff \mathcal{D}(x) = x\oplus g, \quad g \triangleq \mathcal{D}(\mu)$$

Thus any DTI system is equivalent to a morphological dilation of the input with its impulse response. Further, $\mathcal{D}$ is causal iff $g(t) = -\infty \ \forall t < 0$ and stable iff $\sup\{|g(t)| : t \in \mathrm{Spt}(g)\} < \infty$.

Operators $\mathcal{E} : x \mapsto y = \mathcal{E}(x)$ that are time-invariant and obey an infimum superposition, i.e. as in (1) but with $\bigvee$ replaced by $\bigwedge$, are called *erosion translation-invariant (ETI)* systems. These are equivalent to a morphological erosion, because $\mathcal{E}$ is ETI iff $\mathcal{E}[x(t)] = x(t)\ominus f(-t)$, where $f = \mathcal{E}(-\mu)$ is defined as their impulse response.

To describe the time dynamics of DTI systems we also develop nonlinear difference equations. Inspiration here comes from the linear difference equations which can describe a very large class of discrete linear time-invariant (LTI) systems. Replacing sum with maximum and multiplication with addition gives us the following **max difference equation**

$$y[n] = \left(\bigvee_{k=1}^{N} a_k + y[n-k]\right) \vee \left(\bigvee_{m=0}^{M} b_m + x[n-m]\right) \qquad (2)$$

All coefficients a_k, b_m are from $\mathbf{R} \cup \{-\infty\}$. N is the order of the equation, assuming $a_N > -\infty$. The vast majority of discrete-time morphological dilations used in applications employs a finite structuring element, and they can be modeled by (2) by ignoring the recursive part (i.e., if all $a_k = -\infty$). The only exception is the 1st-order recursive dilation $y[n] = \max(y[n-1] - 1,\ x[n])$, which can generate the distance transform of binary images, useful for image analysis. Whenever the max equation has a recursive part, we show that this corresponds to dilating the input signal with an infinite-support structuring function.

To create a **transform domain** for morphological systems, after finding that the line signals $\alpha t + b$ are their eigenfunctions, we introduce a 'slope response', a function of the slope variable α, which enables us to understand the systems behavior in a transform domain–the slope domain. The

Early parts of this research work were partially supported by the US National Science Foundation under Grant MIP–8658150. This paper was written while the author was supported by National Science Foundation under Grant MIP–9396301.

affine signals $x(t) = \alpha t + b$ are *eigenfunctions* of any DTI system $\mathcal{D}$ or ETI system $\mathcal{E}$ because

$$\mathcal{D}[\alpha t + b] = \alpha t + b + G(\alpha) \quad , \quad G(\alpha) \triangleq \bigvee_t g(t) - \alpha t$$

$$\mathcal{E}[\alpha t + b] = \alpha t + b + F(\alpha) \quad , \quad F(\alpha) \triangleq \bigwedge_t f(t) - \alpha t$$

We call the corresponding eigenvalues $G(\alpha)$ and $F(\alpha)$ the **slope response** of the DTI and ETI system. It measures the amount of shift in the intercept of the input lines with slope α. It is also conceptually similar to the frequency response of LTI systems which is their multiplicative eigenvalue for input exponentials, whereas G (or F) is the additive eigenvalue of DTI (or ETI) systems for input lines. This nonlinear analysis leads to developing signal transforms called *slope transforms* whose properties and application to morphological systems has some striking conceptual similarities with Fourier transforms and their application to LTI systems.

This paper is a summary of our results in [3, 4, 5].

2. SLOPE TRANSFORMS

The following two (sup/inf-based) slope transforms, originally introduced by Maragos [3, 4, 5] in the context of morphological systems, were motivated by the algebraic expression of their eigenvalues corresponding to their eigenfunctions $\alpha t + b$. (Recall that the Fourier transform can be similarly inspired by the form of the eigevalues (frequency response) of LTI systems corresponding to their exponential eigenfunctions.) Thus, viewing the slope response as a signal transform with variable the slope α, we define for any signal $x(t)$ its **upper slope transform** as the function $X_\vee : \mathbf{R} \to \overline{\mathbf{R}}$ and as **lower slope transform**[1] the function $X_\wedge : \mathbf{R} \to \overline{\mathbf{R}}$ defined, for each $\alpha \in \mathbf{R}$, as

$$X_\vee(\alpha) \triangleq \bigvee_{t \in \mathbf{R}} x(t) - \alpha t \quad , \quad X_\wedge(\alpha) \triangleq \bigwedge_{t \in \mathbf{R}} x(t) - \alpha t$$

A geometrical intuition behind the slope transforms can be obtained by realizing that a line that has *slope* α and passes from a point $(t, x(t))$ on the graph of a signal $x(t)$ has an *intercept* equal to $X = x(t) - \alpha t$. Thus the upper and lower slope transforms are the max and min intercepts of lines with varying slopes intersecting the signal's graph. These extreme intercepts occur when the line becomes tangent or intersects the graph at only one point. In general, $x(t)$ is covered from above by all the lines $X_\vee(\alpha) + \alpha t$ whose infimum creates an *upper envelope* $\hat{x}(t)$ and is covered from below by all the lines $X_\wedge(\alpha) + \alpha t$ whose supremum creates the *lower envelope* $\check{x}(t)$:

$$\hat{x}(t) \triangleq \bigwedge_{a \in \mathbf{R}} X_\vee(\alpha) + \alpha t \quad , \quad \check{x}(t) \triangleq \bigvee_{a \in \mathbf{R}} X_\wedge(\alpha) + \alpha t$$

We view the signals $\hat{x}(t)$ and $\check{x}(t)$ as the 'inverse' upper and lower slope transform of $x(t)$, respectively.

Theorem 1 [5]. *For any signal* $x : \mathbf{R} \to \overline{\mathbf{R}}$,
(a) $X_\vee(\alpha)$ *and* $\check{x}(t)$ *are convex, whereas* $X_\wedge(\alpha)$ *and* $\hat{x}(t)$ *are concave. (b) For all* t, $\check{x}(t) \le x(t) \le \hat{x}(t)$.
(c) At any time instant t

$$\hat{x}(t) = x(t) \iff x(t) \ge \frac{px(t-q) + qx(t+p)}{p+q} \quad \forall p, q > 0. \tag{3}$$

At any t, $x(t) = \check{x}(t)$ *iff the* $\ge$ *sign in* (3) *is replaced by* $\le$.
(d) $\hat{x}(t) = x(t)$ *for all* t *if* x *is concave, and* $\check{x} = x$ *if* x *is convex. (e)* $\hat{x}$ *is the smallest concave upper envelope of* x, *and* $\check{x}$ *is the greatest convex lower envelope of* x.

Thus, there is one-to-one correspondence between $X_\vee(\alpha)$ and the signal envelope $\hat{x}(t)$. However, all signals between $x(t)$ and $\hat{x}(t)$ will have the same upper slope transform.

Tables I and II list several properties and examples of the upper slope transform. Their proofs are in [5]. The most striking is Property 8, i.e., that dilation in the time domain corresponds to addition in the slope domain. Note the analogy with LTI systems where convolving two signals in time corresponds to multiplying their Fourier transforms.

Consider the rectangular time pulse $w(t)$, equal to 0 for $t \le |T|$ and $-\infty$ else, added to a signal $x(t)$. The upper slope transform of the time-limited signal $x(t) + w(t)$ is the erosion of the original signal's slope transform $X(\alpha)$ by the negative of the window's slope transform $W(\alpha) = T|\alpha|$. See Fig. 1. This is a kind of nonlinear blurring. Consider the analogy with the blurring that occurs when we multiply a signal x by a time window in which case the original Fourier transform of x is convolved with the window's Fourier transform.

There is a duality between the time and slope domain, similar to the duality between time and frequency domains of Fourier transform pairs. For example, Table II implies that time lines, half-lines, and cones transform respectively into slope impulses, steps, and pulses, and vice-versa.

Whatever we discussed for upper slope transforms also applies to the lower slope transform, the only differences being the interchange of suprema with infima, concave with convex, and dilation with erosion.

For **differentiable** signals, the maximization or minimization of the intercept $x(t) - \alpha t$ involved in both slope transforms can also be done, for a fixed α, by finding its value at the stationary point t^* such that $x'(t^*) = \alpha$ where $x' = dx/dt$. At the point $(t^*, x(t^*))$ the line becomes tangent to the graph. This extreme value of the intercept (as a function of the slope α) is the Legendre transform of the signal x:

$$X_L(\alpha) \triangleq x\left((x')^{-1}(\alpha)\right) - \alpha[(x')^{-1}(\alpha)]$$

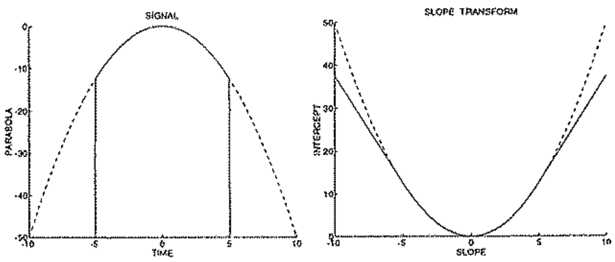

(a) (b)

Figure 1. (a) Original parabola signal $x(t) = -t^2/2$ (in dashed line) and a time-limited version (in solid line) resulting from adding to the signal a rectangular pulse with support $[-5, 5]$. (b) Upper slope transform of the parabola (in dashed line) and of its time-limited version (in solid line).

[1] In convex analysis [8], given a convex function h there uniquely corresponds another convex function $h^*(\alpha) = \bigvee_t \alpha t - h(t)$ called the *conjugate* of h. The lower slope transform of h and its conjugate function are closely related since $h^*(\alpha) = -H_\wedge(\alpha)$.

where f^{-1} denotes the inverse of a function f. It is extensively used in mathematical physics [1]. If the signal $x(t)$ is concave or convex and has an invertible derivative, its Legendre transform is single-valued and equal (over the slope intervals it is defined) to the upper or lower transform. Examples 7–12 deal with such signals x with invertible derivatives.

If a differentiable signal is neither convex nor concave or if it does not have an invertible derivative, the Legendre transform is multi-valued; i.e., $(x')^{-1}(\alpha)$ and hence $X_L(\alpha)$ is a set of real numbers for each α. For example, consider the cosine $x(t) = \cos(\omega_0 t)$ over all time, which is an infinite sequence of convex and concave cosine pulses. Then

$$X_L(\alpha) = \{Y(\alpha)+\alpha kT, -Y(\alpha)+\alpha T(k-0.5) : k = 0, \pm 1, \pm 2, ...\}$$

where Y is the slope transform of a single concave cosine pulse (Example 12, Table II). In general, the number of different functions in the multivalued Legendre transform is equal to the number of consecutive convex and concave pieces making up the signal. This could be finite or infinite. This multivalued Legendre transform is defined in [2] as a 'slope transform' and is expressed via stationary points; i.e., $X_L(\alpha) = \{x(t^*) - \alpha t^* : x(t^*) = \alpha\}$. Its properties in [2] seem similar to the properties of the upper/lower slope transform, but there are some important differences (see [4, 5]) stemming from the fact that operations among multivalued Legendre transforms are actually set operations.

An arbitrary signal can be analyzed using slope transforms toward at least two different goals: signal reconstruction, or envelope reconstruction. For exact signal reconstruction, we should segment the signal into consecutive convex and concave pieces and find the slope transform of each piece. The set collection of slope transforms of the signal pieces can reconstruct the signal exactly. The disadvantage here is the multivaluedness of the transform. Alternatively, for extracting information about the long-time behavior of the signal, as manifested by its upper and lower envelope, we could compute its upper and lower slope transforms and take their inverses, which give us the two envelopes. Examples of this latter case include the impulse responses of recursive DTI systems (discussed later) and amplitude-modulated signals where we seek to estimate their envelope.

Consider **sampling** a continuous-time signal $x_c(t)$ at time instants $t = nT$ and obtaining the sampled signal $x_s(t) = \bigvee_n x[n] + \mu(t - nT)$, where $x[n] = x_c(nT)$ is the **discrete-time** signal. Let $X_c(\alpha)$, $X_s(\alpha)$ be the continuous-time upper slope transforms of the signals $x_c(t), x_s(t)$. We define the upper slope transform of the discrete signal $x[n]$ by

$$X_d(\alpha) \triangleq \bigvee_{n=-\infty}^{\infty} x[n] - \alpha n \quad , \quad \alpha \in \mathbb{R}.$$

Then $X_d(\alpha) = X_s(\alpha/T) \leq X_c(\alpha/T)$.

Another effect of sampling is to replace parts of the slope transform of the continuous-time signal with supporting lines. Further, if $x_c(t)$ is a concave piecewise-linear signal and the sampling time instants $t = nT$ include all the times at which its corner points occur, then $X_c(\alpha) = X_s(\alpha)$ for all α and the original signal $x_c(t)$ can be exactly reconstructed from its samples by applying an upper slope transform on $x_s(t)$ followed by its inverse transform.

The definitions and (almost all) properties of discrete upper and lower slope transforms and their inverses are identical to the continuous-time case, except that the time variable is discrete. Examples 1–6 of slope transform pairs in Table II also hold in discrete time.

3. MAX DIFFERENCE EQUATIONS

In this section we consider discrete-time signals and view (2) as a nonlinear system $\Psi : x \mapsto y = \Psi(x)$. To solve (2) in forward time $n \geq n_0$ we need N *initial conditions* $IC[n_0]$, where $IC[n] = \{y[n-1], y[n-2], ..., y[n-N]\}$. If all the values in $IC[n_0]$ are $-\infty$, the initial state of the system does not affect its output. We define the *impulse response* g of Ψ as its output when the input is the impulse and $IC[0] = -\infty$. The solution of the 1st-order ($N = 1$, $M = 0$) max equation (2) is found by induction on $n \geq 0$ to be

$$y[n] = (x[n] \oplus g[n]) \vee (a_1(n+1) + y[-1])$$

where $g[n] = a_1 n + b_0 + \lambda[n]$ is the impulse response. Thus the general solution of (2) for $N = 1$ is the maximum of the $(-\infty)$-state response (i.e., the dilation $x \oplus g$) and the $(-\infty)$-input response due only to the initial condition $y[-1]$. The system is stable only if $a_1 = 0$. Similar results are also true for the general N^{th}-order max difference equation.

Theorem 2 [4]. *The max difference equation* (2) *corresponds to a causal DTI system if (i) whenever $x[n] = -\infty$ for all $n < n_0$ then $y[n] = -\infty$ for all $n < n_0$, where n_0 is an arbitrary but otherwise fixed time instant, and (ii) the required initial conditions $IC[n_0]$ are $-\infty$.*

Henceforth we shall make the two assumptions of Theorem 2 for systems described by (2). There are two major subclasses of such DTI systems:

Finite Impulse Response (FIR) DTI systems, when $a_k = -\infty$ for all k. Then (2) has no recursive part, and the impulse response has finite support because $g[n] = b_n$ if $n = 0, 1, ..., M$ and $g[n] = -\infty$ else. All these systems are stable. This class is identical with the class of all morphological dilations with finite-support structuring elements.

Infinite Impulse Response (IIR) DTI systems, when $a_k \neq -\infty$ for at least one k. The example of the 1st-order system demonstrates that such systems have an impulse response of infinite support. Their stability is controlled by the max absolute value of g.

Henceforth, we focus only on the recursive part of (2) by setting $b_0 = 0$ and $b_m = -\infty$ for $m > 0$. A 1st-order system $y[n] = \max(y[n-1] + a_1, x[n])$ has impulse response $g[n] = a_1 n + \lambda[n]$ and slope response $G(\alpha) = -\lambda(\alpha - a_1)$. It acts as a *'slope highpass' filter* since it passes from the input signal only those segments whose upper slopes are $\geq a_1$. For a system order $N > 1$, finding a closed-formula expression for the impulse response is generally not possible. However, we can first find the slope response G and then, via inverse slope transform, find the impulse response g or its envelope $\hat{g}$. Thus, applying upper slope transform to (2) and using the fact that $Y_\vee(\alpha) = G(\alpha) + X_\vee(\alpha)$ yields

$$G(\alpha) = \max\{G(\alpha) - \alpha + a_1, ..., G(\alpha) - N\alpha + a_N, \ 0\}$$

A nontrivial (i.e., different than ∞) solution G is

$$G(\alpha) = -\lambda(\alpha - \alpha_0) \quad , \quad \alpha_0 = \max_k \frac{a_k}{k}$$

The inverse slope transform on G yields the upper envelope $\hat{g}$ of the impulse response

$$\hat{g}[n] = \alpha_0 n + \lambda[n] \geq g[n]$$

Over short time periods g has the shape induced by the sequence $\{a_k\}$ and dominates the output of the recursive DTI system during time periods when the slope of the input signals is smaller than α_0. But over time scales much longer than the length of the coefficient sequence $\{a_k\}$ it behaves like its upper envelope $\hat{g}$. Together G and $\hat{g}$ can describe the long-time dynamics of the system where they predict a behavior approximately equivalent to a 1st-order system whose cutoff slope is α_0. In addition, if g is a line, then the above analysis is also exact for the short-time behavior. Note also that by appropriately choosing the coefficients $\{a_k\}$ we can give the short-time variations of g many different patterns, even periodic [3, 4].

3.1. SLOPE FILTERS

Consider the causal recursive DTI system $y_1[n] = \max(y_1[n-1] + a_1, x[n])$ with $a_1 < 0$, which is a morphological dilation of the input by the causal line $g_1[n] = a_1 n + \lambda[n]$. The output $y_1[n]$ provides a type of upper envelope of $x[n]$. As Fig. 2 shows, when computing y_1 in forward time, during periods where the signals peaks keep decreasing y_1 falls linearly with slope a_1 in between these consecutive peaks. When the envelope peaks start increasing, y_1 continues to fall between peaks, whereas it should rise. The slope response of this system is $G_1(\alpha) = -\lambda(\alpha - a_1)$ and hence rejects all negative slopes $< a_1$. To be able to also reject some positive slopes we must pass the input through an anti-causal system $y_2[n] = \max(y_2[n+1] + a_2, x[n])$ with $a_2 > 0$, run backwards in time (see Fig. 2). It corresponds to a morphological dilation of the input by the anti-causal line $g_2[n] = a_2 n + \lambda[-n]$. Its slope response is $G_2(\alpha) = -\lambda(a_2 - \alpha)$ and hence it rejects all positive slopes $> a_2$. To symmetrize this process we can take the maximum $y = y_1 \vee y_2$ of the two envelopes as the final estimated upper envelope of the input. The mapping $x \mapsto y$, i.e., the maximum of two DTI systems, is another DTI system with overall impulse response $g = g_1 \vee g_2$ and overal slope response $G = G_1 \vee G_2$:

$$g[n] = \begin{cases} a_1 n, & n \geq 0 \\ a_2 n, & n \leq 0 \end{cases} \quad , \quad G(\alpha) = \begin{cases} 0, & a_1 \leq \alpha \leq a_2 \\ +\infty, & \text{else} \end{cases}$$

This is an ideal-cutoff *bandpass slope-selective* filter. To design a *symmetric* slope filter we select $a_2 = -a_1 = \alpha_0 > 0$ which passes upper slopes with magnitude $\leq \alpha_0$ unchanged and rejects all other slopes. This is the case in Fig. 2. Such bandpass slope filters, implemented via 1st-order recursive max/min equations, have been applied to envelope detection from AM signals in [3, 4].

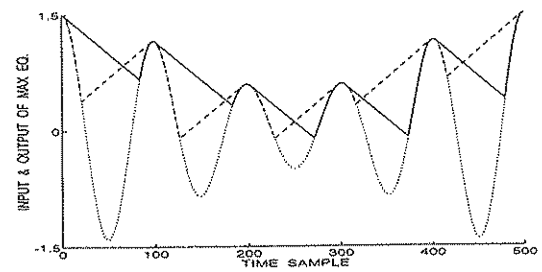

Figure 2. Dotted line shows input signal $x[n] = [1 + 0.5\cos(2\pi n/500)]\cos(2\pi n/100)$. The solid (resp. dashed) line is the output of the recursive equation $y[n] = \max(y[n-1] \pm 0.01, x[n])$ run in forward (resp. backward) time. Final upper envelope is the max of the solid and dashed curves.

4. REFERENCES

[1] R. Courant and D. Hilbert, *Methods of Mathematical Physics*, Wiley, NY, 1962.

[2] L. Dorst and R. van den Boomgaard, "An Analytical Theory of Mathematical Morphology", in *Proc. 1st Int'l Workshop on Math. Morphology and its Application to Signal Processing*, Barcelona, Spain, May 1993.

[3] P. Maragos, "Max-Min Difference Equations and Recursive Morphological Systems", in *Proc. 1st Int'l Workshop on Math. Morphology and its Application to Signal Processing*, Barcelona, Spain, May 1993.

[4] P. Maragos, "Morphological Systems: Slope Transforms and Max–Min Difference and Differential Equations", *Signal Processing*, Sep. 1994.

[5] P. Maragos, "Slope Transforms: Theory and Application to Nonlinear Signal Processing", submitted to IEEE Trans. on Signal Processing.

[6] P. Maragos and R. W. Schafer, "Morphological Systems for Multidimensional Signal Processing", *Proc. IEEE*, vol. 78, pp. 690-710, Apr. 1990.

[7] J. Serra, *Image Analysis and Mathematical Morphology*, NY: Acad. Press, 1982.

[8] J. van Tiel, *Convex Analysis*, NY: Wiley, 1984.

TABLE I: Properties of Upper Slope Transform

No.	Signal: $x(t)$	Transform: $X_\vee(\alpha)$
1.	$\bigvee_i c_i + x_i(t)$	$\bigvee_i c_i + X_i(\alpha)$
2.	$x(t - t_0)$	$X(\alpha) - \alpha t_0$
3.	$x(t) + \alpha_0 t$	$X(\alpha - \alpha_0)$
4.	$x(rt)$	$X(\alpha/r)$
5.	$x(-t)$	$X(-\alpha)$
6.	$x(t) = x(-t)$	$X(\alpha) = X(-\alpha)$
7.	$rx(t)\ ,\ r > 0$	$rX(\alpha/r)$
8.	$x(t) \oplus y(t)$	$X(\alpha) + Y(\alpha)$
9.	$\bigvee_\tau x(\tau) + y(t+\tau)$	$X(-\alpha) + Y(\alpha)$
10.	$x(t) \leq y(t)\ \ \forall t$	$X(\alpha) \leq Y(\alpha)\ \ \forall \alpha$
11.	$x(t) \leq X(0)\ \ \forall t$	$X(\alpha) \geq x(0)\ \ \forall \alpha$
12.	$y(t) = \begin{cases} x(t), & \lvert t\rvert \leq T \\ -\infty, & \lvert t\rvert > T \end{cases}$	$Y(\alpha) = X(\alpha) \ominus (-T\lvert\alpha\rvert)$

TABLE II: Examples of Upper Slope Transforms

No.	Signal: $x(t)$	Transform: $X_\vee(\alpha)$
1.	$\alpha_0 t$	$-\mu(\alpha - \alpha_0)$
2.	$\alpha_0 t + \lambda(t)$	$-\lambda(\alpha - \alpha_0)$
3.	$\mu(t - t_0)$	$-\alpha t_0$
4.	$\lambda(t - t_0)$	$-\alpha t_0 - \lambda(\alpha)$
5.	$\begin{cases} 0, & \lvert t\rvert \leq T \\ -\infty, & \lvert t\rvert > T \end{cases}$	$T\lvert\alpha\rvert$
6.	$-\alpha_0\lvert t\rvert,\ \ \alpha_0 > 0$	$\begin{cases} 0, & \lvert\alpha\rvert \leq \alpha_0 \\ \infty, & \lvert\alpha\rvert > \alpha_0 \end{cases}$
7.	$\sqrt{1 - t^2},\ \ \lvert t\rvert \leq 1$	$\sqrt{1 + \alpha^2}$
8.	$-t^2/2$	$\alpha^2/2$
9.	$-\lvert t\rvert^p/p\ ,\ p > 1$	$\lvert\alpha\rvert^q/q\ ,\ 1/p + 1/q = 1$
10.	$\exp(t)$	$\alpha[1 - \log(\alpha)]$
11.	$\tanh(t),\ \ t \geq 0$	$\sqrt{1 - \alpha} - \alpha \log\left(\frac{1 + \sqrt{1-\alpha}}{\sqrt{\alpha}}\right)$
12.	$\cos(\omega_0 t),\ \ \lvert t\rvert \leq \frac{\pi}{2\omega_0}$	$\sqrt{1 - \frac{\alpha^2}{\omega_0^2}} + \left(\frac{\alpha}{\omega_0}\right)\sin^{-1}\left(\frac{\alpha}{\omega_0}\right)$